ELSEVIER

Biophysical Chemistry 79 (1999) 1–9

Biophysical Chemistry

Paramagnetic fluorescence quenching in a model membrane: a consideration of lifetime and temperature

David A. Johnson*, Binh Nguyen, Anibal F. Bohorquez, C. Fernando Valenzuela[1]

Division of Biomedical Sciences, University of California, Riverside, CA 92521-0121, USA

Received 22 December 1998; accepted 3 January 1999

Abstract

To expand our understanding of paramagnetic quenching in membranes, the relationship between fluorophore excited-state lifetime (τ), temperature, and the collisional quenching was studied. Specifically, the ability of tempo to quench the steady-state and time-resolved emission from five lipophilic fluorophores (diphenylhexatriene, perylene, phenanthrene, pyrene, and triphenylene) partitioned into egg phosphatidylcholine (EggPC) liposomes was examined. Also, the temperature dependence of spin-labeled androstane to quench the emission (steady-state and time-resolved) from perylene in EggPC liposomes was determined. Unexpectedly, in EggPC liposomes, the apparent quenching efficiency decreased with increasing τ until the effect leveled off above $\sim$20 ns. Moreover, in EggPC liposomes, dynamic quenching decreased with increasing temperature. The results suggest that in membranes, paramagnetic quenching is more complex than generally recognized.

Keywords: Paramagnetic fluorescence quenching; Fluorescent probe; Spin label; Liposomes; Time-resolved fluorescence

1. Introduction

Molecular interactions in biological membranes have been increasingly studied by means of fluorescence quenching with stable nitroxyl free radicals (spin-labels). Examples of the issues pursued by paramagnetic quenching with spin-labels include: the determination of the affinity of lipids toward membrane proteins [1], the assessment of the transverse position of intrinsic and extrinsic fluorophores [2–4], the evaluation of lipid phase separation [5], and the localization of ligand-binding sites on receptors [6–10].

It has been recognized for some time that no matter what the excited-state lifetime (τ) of the fluorophore is, spin-label-induced quenching in

Abbreviations: ASL, 5-doxyl-17β-hydroxy-5α-androstane; DPH, 1,6-diphenyl-1,3,5-hexatriene; EggPC, Egg phosphatidylcholine; tempo, 2,2,6,6-tetramethylpiperdine-1-oxyl.

* Corresponding author. Tel.: +1-909-787-3831; fax: +1-909-787-5504; e-mail: david.johnson@ucr.edu

[1] Present address: Department of Neuroscience, University of New Mexico HSC, Albuquerque, NM 87131

0301-4622/99/$ - see front matter
PII: S0301-4622(99)00036-8

non-viscous, isotropic solvents will display both dynamic (reduced fluorescence lifetime) and static (loss of fluorescence without changes in fluorescence lifetime) components. In lipid membranes, on the other hand, the situation is more complex. Up until about a decade ago, it has been generally assumed that spin-label-induced quenching in membranes is only static for fluorophores with excited-state lifetimes of less than $\sim 20-50$ ns. The reason for this assumption is that dynamic quenching (not involving dipolar energy transfer) is diffusion-dependent and that fluorophore/quencher translational diffusion in membranes is too slow (10^7-10^8 cm^2/s) to produce a significant number of collisions within the duration of the excited state of the fluorophore [1]. However, Merkle et al. [11] demonstrated that spin-label-induced dynamic quenching, in fact, occurs in membranes with short-lived fluorophores. Fast local motions (i.e. wobbling, rotation, *gauche-trans* isomerization, vertical fluctuations) of the spin-label and/or the fluorophore are postulated to allow for this dynamic quenching [11,12].

Short-lived lipophilic fluorophores should, therefore, have the capacity to monitor fast motions of membrane-associated fluorophores and spin-labels and, thus, provide additional uses for paramagnetic quenching. While the experimental support for this local-motion hypothesis is compelling, the phenomena have not been completely characterized. For example, it is unclear whether there is a unique relation between the τ and the quenching. Also, the effect of temperature on this quenching has not been examined.

Consequently, to expand our understanding of paramagnetic quenching in membranes, we examined in detail the relation between fluorophore lifetime and temperature on paramagnetic quenching. Specifically, the differential ability of a spin-label, tempo, to quench the emission (steady-state and time-resolved) from five lipophilic fluorophores (diphenylhexatriene (DPH), perylene, phenanthrene, pyrene, and triphenylene) that were partitioned into egg phosphatidylcholine (EggPC) liposomes was examined. Also, the temperature dependence of spin-labeled androstane (ASL) to quench the emission (steady-state and time-resolved) of one of these fluorophores (perylene) was determined to assess whether or not dynamic quenching increased with temperature as generally assumed. Two novel observations about paramagnetic quenching in model membranes were made: (1) the apparent bimolecular collision rates for the series of fluorophores decreased with increasing τ until it leveled off above ~ 20 ns, and (2) dynamic quenching decreases with increasing temperature. The results appear to suggest a greater complexity to paramagnetic quenching in membrane than is generally recognized.

2. Materials and methods

2.1. Materials

Triphenylene, perylene, phenanthrene, and 2,2,6,6-tetramethylpiperdine-1-oxyl (tempo) were obtained from Aldrich Chemical Co. (Milwaukee, WI). 1,6-diphenyl-1,3,5-hexatriene (DPH) was purchased from Molecular Probes (Eugene, OR). Pyrene was obtained from Sigma Chemical Co. (St. Louis, MO). EggPC was purchased from Calbiochem (La Jolla, CA.).

2.2. Preparation of EggPC liposomes

Multilamellar lipid dispersions were made by dissolving EggPC in a 1:1 methanol/chloroform mixture and rotary evaporating the mixture until dry. The sample was then placed under a vacuum (< 1 mtorr) for at least 30 min. The thin film was then hydrated with warm 10 mM $NaPO_4$, pH 7.4 (Buffer I) and vortexed for 5 min in the presence of glass beads.

2.3. Fluorescence measurements

Steady-state fluorescence measurements were made with a Perkin-Elmer Cetus MPF 66 spectrofluorometer. Fluorescence lifetimes were determined by the time-correlated single-photon counting technique using an EEY Scientific nanosecond spectrofluorometer (La Jolla, CA.) equipped with a high pressure hydrogen arc lamp. All titration were carried out in 0.5×0.5-cm cuvettes, under argon, and at room temperature

unless stated otherwise. Fluorescence values were corrected for dilution as a result of added titrant and the intrinsic absorbance of the sample as described by Valenzuela et al. [6]. Fluorescence decay data was analyzed with Globals Unlimited computer program (Laboratory of Fluorescence Dynamics, Urbana, IL.).

For the lifetime measurements excitation and emission wavelengths were selected for the various fluorophores with the following filter combinations (excitation, emission): perylene (Oriel 400 nm broad-band interference, Corning 3–71 cuton), DPH (Oriel 340-nm interference, Oriel 450-nm broad-band interference), triphenylene (Oriel 280-nm interference, Oriel 59459 cuton), phenanthrene (Oriel 290-nm interference, Oriel 59460 cuton), and pyrene (Oriel 340-nm interference, Schott KV-389 cuton). Pyrene fluorescence was always measured with the sample under a nitrogen atmosphere to minimize oxygen quenching.

2.4. Fluorescence quenching by tempo in cyclohexane

All stock solutions of fluorophores and tempo were initially dissolved in cyclohexane except for DPH, which was dissolved in methanol. Fluorophores were added to argon-saturated cyclohexane to give a final concentration of 6 μM. Tempo (1 M) was added to the cuvettes with a Hamilton syringe. Fluorescence lifetimes were measured before and after the addition of tempo.

The results were initially fit to the Stern–Volmer equation

$$\tau_o/\tau = 1 + K_Q[Q] \quad (1)$$

where τ_0 and τ are the fluorescence lifetimes of the fluorophores in the absence and presence of a concentration $[Q]$ quencher, respectively. K_Q, the Stern–Volmer quenching constant is related to the apparent bimolecular collision rate constant (k_q) by the expression

$$k_q = K_Q/\tau_o. \quad (2)$$

In cyclohexane, where the bimolecular collision rate constant (k_o) can be estimated with the Smoluchowski equation, the quenching efficiency (γ) or the quenching probability per encounter can be calculated with the expression

$$\gamma = k_q/k_o. \quad (3)$$

2.5. Paramagnetic quenching in EggPC liposomes

The fluorophores (6 μM) were added to a suspension of EggPC liposomes (600 μM) and incubated at room temperature for at least 90 min prior to the start of each titration. The effects of scattering were subtracted by measuring the apparent emission from samples that included all the ingredients except the fluorophore. Corrections were also made for dilution and inner filter effects of the spin label. Samples containing DPH were protected from light. The effects of the quencher upon both the steady-state and time-resolved emission were measured and the data were plotted (Stern–Volmer plot) as either steady-state intensity in the absence of quencher over the intensity in the presence of quencher or τ_0/τ vs. quencher concentration. The slopes of these plots are equal to the steady-state (K_Q^{SS}) and time-resolved (K_Q) Stern–Volmer quenching constants, respectively.

3. Results

3.1. Determination of intrinsic quenching efficiency of fluorophores

To have a more detailed understanding of the quenching characteristics of the fluorophores under study, the quenching efficiency of tempo to dynamically quench the emission of the fluorophores was determined in an isotropic medium, cyclohexane. Cyclohexane was chosen because: (i) its hydrocarbon composition is similar to the membrane core; (ii) all the fluorophores under study are soluble in it; and (iii) its isotropic character provides a directionally independent quenching, which presumably should yield a more accurate estimate of the relative quenching efficiencies of the fluorophores.

In cyclohexane the emission decays of DPH, perylene, and pyrene were well fit to a single

exponential equation, while those of phenanthrene and triphenylene were best fit to a biexponential equation (data not shown). Because of the complexity of the phenanthrene and triphenylene emission decays, the geometric average of the two lifetimes was utilized to calculate the bimolecular collision rate constants. The time-resolved Stern–Volmer plots for tempo to shorten (quench) the excited-state lifetimes of the fluorophores examined are shown in Fig. 1. The slopes (K_Q) of linear least-squares fits to these plots along with the apparent collisional rate constants (k_q) and the quenching efficiencies (γ) are presented in Table 1. All the plots were linear and the apparent bimolecular collisional rate constants ranged between 0.46 and 1.5×10^{10} M^{-1} s^{-1}, consistent with a simple diffusion-controlled quenching process. The estimated quenching efficiencies, γ, which are the apparent collisional rate constants divided by the theoretical bimolecular association rates (determined with the Smoluchowski expression), ranged between 0.7 and 2.2 and were in the rank order of DPH = perylene > pyrene > triphenylene > phenanthrene. The greater than unity value of these quenching efficiencies is consistent with the effective encounter distance of the spin label extending a few angstroms beyond its van der Waals radius [13]. Also, the threefold variation in these quenching efficiencies shows that tempo is not equally effective in quenching all fluorophores even when the chemical compositions of the fluorophores are relatively similar. And, not surprisingly, no correlation ($r = -0.1$) between τ and γ was observed, which shows that the excited-state lifetime of the fluorophores is unrelated to the efficacy of a spin label to quench emission in cyclohexane.

Table 1
Summary of the isotropic Stern–Volmer quenching constants, decay rates, apparent collisional rate constants, and quenching efficiencies for tempo quenching the emission from five fluorophores in cyclohexane

Fluorophore	K_Q^a (M^{-1})	τ_0^b (ns)	$k_q \times 10^{-9c}$ (M^{-1} s^{-1})	γ^d
DPH	164	11.5	14.2	2.2
Perylene	65	4.5	14.5	2.2
Phenanthrene	194	42.2[e]	4.6	0.7
Pyrene	2023	180	11.2	1.7
Triphenylene	266	37.9[e]	7.0	1.1

[a] Stern–Volmer quenching constant calculated (Eq. (1)) from the slopes of the data plots in Fig. 1 (Each value represents the mean of 3–5 determinations).

[b] Fluorescence lifetime in cyclohexane in the absence of quencher.

[c] Apparent bimolecular quenching rate constant calculated using Eq. (2).

[d] Quenching efficiency estimated by dividing k_q by k_0, the theoretical association rate for diffusion of the fluorophore and the quencher toward each other calculated with Eq. (3). The values of k_o ranged between 6.54 and 6.57×10^9 M^{-1} s^{-1}.The theoretical k_0 can be estimated with the Smoluchowski equation

$$k_o = (4\pi N/1000)(R_f + R_q)(D_f + D_q)$$

where N is the Avogadro's number, and R and D are the radius and diffusion coefficients of the fluorophore (f) and quencher (q). D can be estimated using the Stokes–Einstein equation

$$D = kT/6\pi\eta R$$

where k is the Boltzmann's constant, T the temperature (°K), and η is the viscosity of the media.

[e] Geometric average lifetime calculated with the expression $\Sigma a_i \tau_i / \Sigma a_i$, where a_i and τ_i are the preexponential term and lifetime of the ith decay component, respectively.

3.2. Paramagnetic quenching in EggPC liposomes

The tempo-induced quenching of both the steady-state and time-resolved emission of the various fluorophores under study were determined and the Stern–Volmer plots of the results are illustrated in Fig. 2. The emission decays of all the fluorophores were complex and best fit to a biexponential equation, Consequently, the geometric averages of the decay parameters were utilized to calculated the bimolecular collision rate constants. Also, to make quantitative comparisons, the total concentration of tempo added at each step of the titrations was used to calculate the apparent quenching constants even though only a fraction of the tempo partitions into the liposomes.

Over the range of quencher concentrations examined all the Stern–Volmer plots were reasonably linear. For the fluorophores examined, the steady-state Stern–Volmer quenching constants

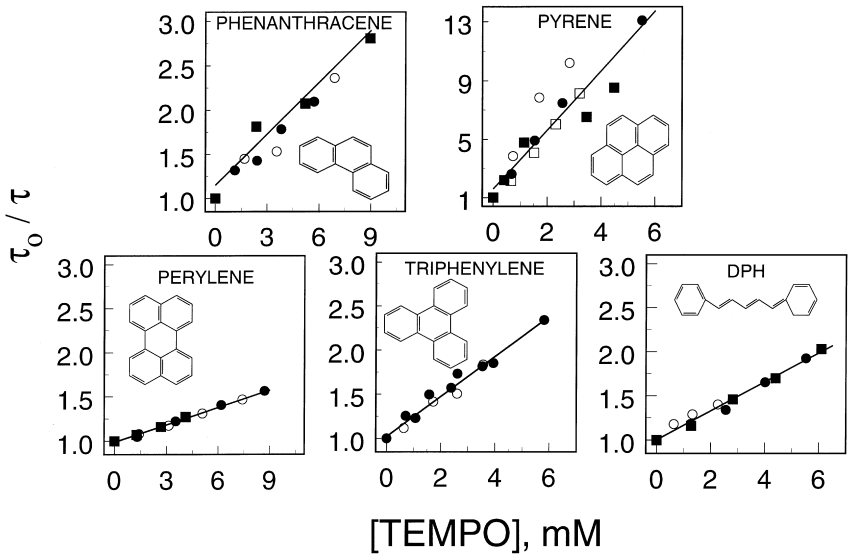

Fig. 1. Stern–Volmer plots for tempo quenching the emission from the five fluorophores in cyclohexane. Quenching is measured as a reduction in the fluorescence lifetime and the various symbols (■, ○, and ●) represents the results of separate experiments. The lines represent linear least-squares fits of the data.

were from 1.1- to 4.6-fold higher than the comparable time-resolved constants (Table 2).

Division of the time-resolved Stern–Volmer quenching constants by the respective lifetimes (Eq. (2)) yields the apparent bimolecular collisional rate constants, k_q's. The descending rank order of these constants is perylene > DPH > phenanthrene > pyrene > triphenylene, which is

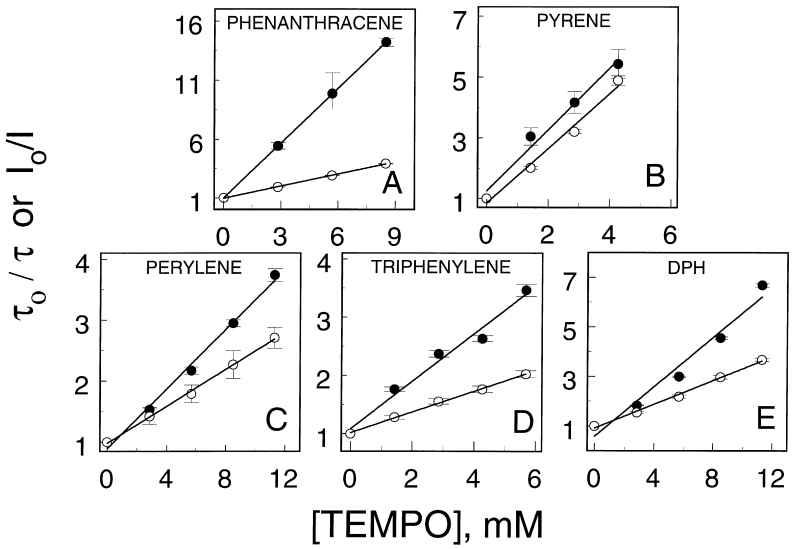

Fig. 2. Stern–Volmer plots for tempo quenching the emission of the five fluorophores in EggPC liposomes. Quenching was measures as either a reduction of the steady-state emission (●) or fluorescence lifetime (○) of the same sample. The error bars represent the S.D. of three determinations. The lines represent linear least-squares fits of the data. The fluorophores (6 μM) were added to multilamellar EggPC liposomes (600 μM) in 10 mM sodium phosphate buffer (pH 7.4) and incubated for 1–2 h at room temperature. Corrections for dilution, intrinsic fluorescence of the sample, and absorbance of the quencher were made in all cases.

Table 2
Summary of the steady-state and time-resolved Stern–Volmer quenching constants, apparent collisional rate constants for tempo quenching of the emission from five fluorophores in EggPC liposomes

	K_Q^{SS} [a] (M^{-1})	K_Q [b] (M^{-1})	$\langle\tau\rangle$ [c] (ns)	$k_q \times 10^{-9}$ [d] ($M^{-1}\ s^{-1}$)	$k_q/\gamma \times 10^{-9}$ [e]
DPH	500	240	7.5	32.3	14.9
Perylene	240	150	2.9	52.1	23.7
Phenanthrene	1600	350	19.7	17.6	25.0
Pyrene	1100	980	105.9	9.3	5.4
Triphenylene	410	180	28.1	6.3	5.9

[a]Apparent Stern–Volmer quenching constant calculated from steady-state quenching data illustrated in Fig. 2.
[b]Apparent Stern–Volmer quenching constant calculated (Eq. (1)) from the slopes of the lifetime quenching data illustrated in Fig. 2.
[c]Geometric average lifetime calculated with the expression $\Sigma a_i\tau_i/\Sigma a_i$, where a_i and τ_i are the preexponential term and lifetime of the ith decay component, respectively.
[d]Apparent bimolecular collision rate constant using Eq. (2) and K_Q.
[e]Apparent bimolecular collision rate constant (k_q) divided by the quenching efficiency (γ) from Table 1.

different from the comparable rank order observed with the fluorophores dissolved in cyclohexane (perylene = DPH > pyrene > triphenylene > phenanthrene). The differential ability of tempo to quench the emission from fluorophores in cyclohexane vs. the hydrocarbon core of EggPC liposomes is quantitatively seen by dividing the EggPC k_q's by the quenching efficiencies, γ, determined in cyclohexane (Table 2). If tempo quenched equaled the emission from fluorophores in both cyclohexane and EggPC liposomes, then the k_q/γ ratios would be about the same, which they are not. These ratios differ from one another by as much as a 4.6-fold. Why these differences occur is unclear but it may reflect differences in the membrane distribution of the fluorophores and/or orientation-dependent differences in their quenching efficiencies.

The relation between the apparent bimolecular collisional rate constant and τ is different in cyclohexane and EggPC liposomes. In cyclohexane, as discussed above, no systematic relation was observed; however, in EggPC liposomes the apparent bimolecular collisional rate constants and, therefore, the relative quenching efficiency decreases with increasing lifetime until the effect levels off above a τ of $\sim$20 ns (Fig. 3). Essentially, this same relationship is seen if the steady-state instead of the time-resolved Stern–Volmer quenching constants are used (data not shown);

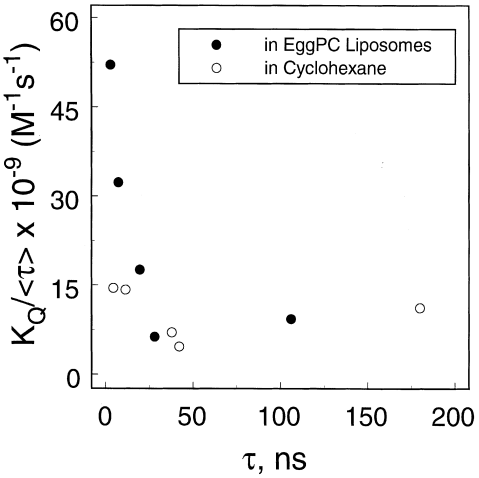

Fig. 3. Relation between the fluorescence lifetime of the fluorophores and their apparent bimolecular rate constants for tempo quenching in EggPC liposomes (●) and in cyclohexane (○).

consequently, this phenomena is unrelated to the static quenching elements in spin-labeled-induced loss of fluorescence.

3.3. Temperature dependence of quenching

To further characterize spin label fluorescence quenching in membranes, the effect of temperature on ASL quenching of the emission from perylene in EggPC liposomes was examined. ASL

was utilized instead of tempo, because the membrane partitioning of tempo can change with temperature. ASL, a steroid, on the other hand, rapidly and essentially completely partitions into membranes at room temperature, and, therefore, its membrane concentration should not vary over the relatively small temperature range (15°C) studied.

The temperature dependence of ASL-induced quenching of both the steady-state and time-resolved emission of perylene was determined, and the results are illustrated in Fig. 4. One set of the Stern–Volmer plots (at 20°C) is shown as an example in the upper panel of Fig. 4. As with the comparable tempo results, the Stern–Volmer plots were essentially linear over the concentration range of ASL examined, and the steady-state data were associated with greater degree of quenching than those obtained from the time-resolved results. Because ASL essentially completely partitions while tempo partially partitions into membranes, the apparent Stern–Volmer quenching constants associated with ASL-induced quenching were ~50-fold greater than those induced by tempo. Significantly, the ratios of the steady-state and time-resolved Stern–Volmer quenching constants were about the same for both spin labels (ASL and tempo), 1.8 (at 20°C) vs. 1.6 (at ~22°C), respectively, indicating that once partitioned into the membrane the two spin labels were equally effective quenchers.

Surprisingly, while there was little or no effect of increasing temperature on the steady-state Stern–Volmer quenching constant, the time-resolved Stern–Volmer quenching constant decreased with increasing temperature (Fig. 4, lower panel). From 15 to 30°C, the dynamic (time-resolved) quenching constant decreased by approximately 36%. This effect cannot be explained by a temperature-dependent increase in the fluorescence lifetime of perylene, because the lifetime of perylene only decreased slightly (4%) as the temperature was increased from 15 to 30°C (data not shown). While it is unclear why this effect occurs, the results are inconsistent with the typical behavior of dynamic quenchers in isotropic environments, where the frequency of collisions and quenching increase with temperature [14].

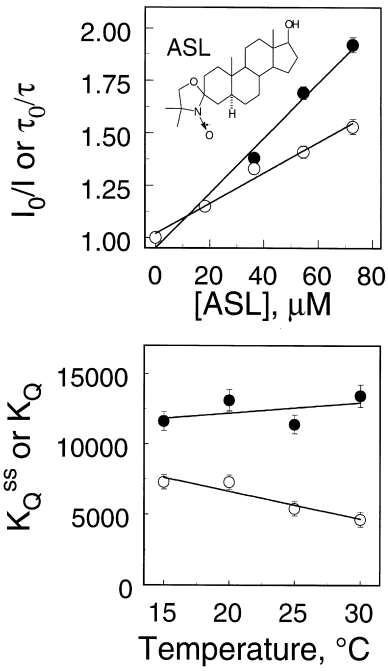

Fig. 4. Temperature dependence of the steady-state and the time-resolved quenching of perylene by ASL in EggPC liposomes. Upper Panel: Stern–Volmer plots of ASL quenching either the steady-state emission (●) or the fluorescence lifetime (○) from perylene (6 μM) partitioned into EggPC liposomes (600 μM) at 20°C. The structure of ASL is shown as an inset. Lower panel: The apparent steady-state (●) and the time-resolved (○) Stern–Volmer quenching constants as a function of temperature for the quenching of perylene emission by ASL in EggPC liposomes. The error bars represent the S.D. of five to six determinations, and the lines represent linear least-squares fits of the data.

4. Discussion

Fluorescence quenching can be dynamic and/or static. Quenching that competes with emission to accelerate the excited-state-to-ground-state relaxation is dynamic and involves either a collision with or resonance energy transfer to a quencher. Quenching that occurs without a change in the fluorescence lifetime of the fluorophore typically involves ground-state phenomena where the quencher either forms a dark complex that absorbs, but does not emit, or a ground-state complex that displays a reduced extinction coefficient relative to the free fluorophore. In non-viscous, isotropic environments

paramagnetic quenchers reduce emission by both dynamic and static mechanisms. Both types of quenching occur with paramagnetic quenchers, because the effective radii of these quenchers extend 4–6 Å beyond their van der Waals radii [13], which effectively prolongs the dwell time of the collisional encounter to produce instantaneous de-excitation and a dark complex.

In this paper, we set out to expand our understanding of paramagnetic quenching by spin labels in membranes. The relationships between τ, temperature, and paramagnetic quenching in EggPC liposomes were explored. Two unexpected observations were made: first, in model membranes, unlike in isotropic media, fluorophores with lifetimes below ~ 20 ns were more effectively quenched by spin labels than those with longer τ's. Second, dynamic quenching decreases with increasing temperature, contrary to the typically observed increase with temperature in isotropic solvents.

The lipid bilayer is an anisotropic medium where lipid movements are much slower than in non-viscous media and are largely constrained to two dimensions. Fluorophores with short excited-state lifetimes should be associated with a shorter period during which an encounter can occur with quenchers, which will proportionally reduce quenching from spin labels at greater distances. The routine division of the observed Stern–Volmer quenching constants by τ to calculate the apparent bimolecular collision rate constant, in essence, compensates for the inherent property of excited-state lifetime to influence the apparent quenching efficiency. Indeed, this compensation eliminates the apparent lifetime dependence of quenching in cyclohexane (Fig. 3), but not in EggPC liposomes. The reason for this phenomenon is unclear. It may some how involve the inherent heterogeneity in the bilayer microenvironment of each fluorophore and thus multiplicity of excited states, each of which with differential sensitivity to paramagnetic quenchers.

The reason for the temperature-dependent decrease in the time-resolved but not steady-state quenching of perylene by ASL in EggPC liposomes is also unclear. For there to be a change in the time-resolved quenching without a change in the steady-state quenching, the dynamic and static components of the quenching must be reciprocally linked, such that as dynamic quenching decreases with increasing temperature static quenching must increase. Because time-resolved emission is only sensitive to dynamic quenching and steady-measurements represent the sum of both static and dynamic quenching, a reciprocal shift from dynamic to static quenching would be observed as a decreasing time-resolved quenching and unchanging steady-state quenching.

This reciprocal shift on the level of dynamic vs. static quenching of perylene emission by ASL could be due to a temperature-dependent redistribution of ASL in the bilayer. This could occur, for example, if the non-polar, disc-shaped perylene distributed primarily between the two bilayer leaflets, parallel to the plane of the bilayer, and the more polar ASL distributed primarily at lower temperatures between phosphatidylcholine molecules, perpendicular to the plane of the bilayer. If elevation of temperature shifted the distribution of ASL toward the middle of the bilayer, then the perylene would increasingly be within the effective encounter distance of ASL and more likely be instantaneously and, therefore, statically quenched.

5. Conclusion

In summary, we found that the quenching efficiency of spin labels has some dependence upon τ ($\tau < 20$ ns) when fluorophores are partitioned into lipid bilayers, but not when dissolved in a non-viscous, isotropic medium like cyclohexane. The reason for this phenomenon is unclear, but may reflect a differential sensitivity of the fluorophores to paramagnetic quenching in the unique microenvironment of a lipid membrane. Additionally, we found that temperature can shift the proportion of dynamic-to-static quenching of perylene emission by ASL. This phenomenon may result from a temperature-dependent redistribution of the ASL from between lipid molecules perpendicular to the plane of the bilayer to the space between the two bilayer leaflets.

Acknowledgements

This work was supported by NSF grant IBN-9515330.

References

[1] E. London, G.W. Feigenson, FEBS Lett. 96 (1978) 51–54.
[2] A. Chattopadhyay, E. London, Biochemistry 13 (1987) 39–45.
[3] A. Chattopadhyay, M.G. McNamee, Biochemistry 30 (1991) 7159–7164.
[4] P.P. Constantinides, Y.Y. Wang, T.G. Burke, T.R. Tritton, Biophys. Chem. 35 (1990) 259–264.
[5] G.W. Feigenson, Biochemistry 22 (1983) 3106–3116.
[6] C.F. Valenzuela, J.A. Kerr, D.A. Johnson, J. Biol. Chem. 267 (1992) 8238–8244.
[7] C.F. Valenzuela, A.J. Dowding, H.R. Arias, D.A. Johnson, Biochemistry 33 (1994) 6586–6594.
[8] H.R. Arias, C.F. Valenzuela, D.A. Johnson, Biochemistry 32 (1993) 6237–6242.
[9] D.A. Johnson, J.M. Nuss, Biochemistry 33 (1994) 9070–9077.
[10] D.A. Johnson, S. Ayres, Biochemistry 35 (1996) 6330–6336.
[11] H. Merkle, W.K. Subczynski, A. Kusumi, Biochim. Biophys. Acta 897 (1987) 238–248.
[12] M.D. Yeager, G.W. Feigenson, Biochemistry 29 (1990) 4380–4392.
[13] J.A. Green, L.A. Singer, J.H. Parks, J. Chem. Phys. 58 (1973) 2690–2695.
[14] J.R. Lakowicz, Principles of Fluorescence Spectroscopy, Plenum, New York, 1983.